Large scale instabilities in two-dimensional magnetohydrodynamics

G. Boffetta,[1] A. Celani,[1] and R. Prandi[2]

[1]*Dipartimento di Fisica Generale, Università di Torino, via Pietro Giuria 1, 10125 Torino, Italy*
and INFM, Unità di Torino, Torino, Italy

[2]*Department of Mathematics, University College London, London WC1E 6BT, United Kingdom,*
and INFM, Unità di Pisa, Pisa, Italy

The stability of a sheared magnetic field is analyzed in two-dimensional magnetohydrodynamics with resistive and viscous dissipation. Using a multiple-scale analysis, it is shown that at large enough Reynolds numbers the basic state describing a motionless fluid and a layered magnetic field, becomes unstable with respect to large scale perturbations. The exact expressions for eddy-viscosity and eddy-resistivity are derived in the nearby of the critical point where the instability sets in. In this marginally unstable case the nonlinear phase of perturbation growth obeys to a Cahn-Hilliard-like dynamics characterized by coalescence of magnetic islands leading to a final new equilibrium state. High resolution numerical simulations confirm quantitatively the predictions of multiscale analysis.

PACS number(s): 52.35.Py, 47.20.Ft

I. INTRODUCTION

The onset of turbulent fluid motion is tightly connected with the appearance of instabilities: a flow pattern sustained by some external forcing is kept in equilibrium by dissipative mechanisms; when dissipative coefficients are lowered below a definite threshold the flow becomes unstable with respect to small amplitude perturbations. Typically, the characteristic length-scale of the perturbations that trigger the instability is smaller than that of the basic flow. The newborn structures are themselves unstable and break into smaller flow patterns, this process eventually generating small-scale fluctuations smoothed out by dissipation. The net effect of the presence of small-scale instabilities is thus an energy drag from large scale structures. This process is usually mimicked by introducing an effective dissipation (eddy viscosity), a very old idea based on the analogy with the derivation of molecular dissipative coefficients in the framework of kinetic theory (see Ref. [1] for a general perspective). Both the former simplified picture and the kinetic analogy dramatically break loose for two-dimensional flows, when instabilities often develop at a scale larger than the one where energy injection takes place. The most renowned example of this phenomenon is observed in the context of the hydrodynamical Kolmogorov flow [2], but other two-dimensional systems like the equivalent-barotropic [3] and the drift-wave [4] models have been proven to exhibit such a phenomenology. In this case, then, the picture drawn above has to be somehow reversed, since larger and larger structures are generated by the chain of instabilities and energy is extracted from smaller scales. Also the kinetic analogy must be revised by introducing the concept of negative eddy viscosity [5] in order to take the inverse energy flux into account.

The purpose of the present paper is to describe the onset of large scale instabilities in two-dimensional magnetohydrodynamics. This phenomenon will be interpreted in terms of a negative eddy resistivity, which in the case under investigation can be analytically derived from the equations of motion by means of multiple scale analysis. The nonlinear phase of the growth of perturbations is also accessible by the same techniques, and numerical simulations provide a precise quantitative assessment of the theoretical results. Eventually the development of large scale perturbations tracks the route to the turbulent inverse cascade of magnetic square potential which characterizes 2D MHD [6].

In Sec. II, we briefly introduce the fluid equations of magnetohydrodynamics and their basic equilibrium states. In Sec. III, the behavior of large scale perturbations is investigated making use of multiple-scale analysis and exact expressions for eddy viscosity and eddy resistivity are derived. The main result is the appearance of large scale transverse instabilities, associated to negative values of the renormalized dissipative coefficients. In Sec. IV, we focus on the case of marginal instability for which we obtain the effective equation for the large scale behavior and we show that the full nonlinear regime is characterized by the evolution towards a fixed point. In Sec. V, we present the results of direct numerical simulations (DNS), which display a clear *quantitative* agreement with the predictions of multiple-scale analysis, both in the linear and in the nonlinear phase.

II. MHD EQUATIONS AND BASIC EQUILIBRIA

MHD equations are relevant in many different physical contests, such as astrophysics, laboratory plasma physics, or magnetized liquid metal dynamics. The applicability of this model, which is a fluid description of plasma, relies on the assumption that all the length scales under consideration must largely exceed the ion Larmor radius. In a strong external magnetic field which is oriented along z, $B_z \gg B_\perp$, the motion becomes almost two-dimensional and the MHD model is well approximated by the 2D MHD equations for the magnetic flux function ψ associated to the planar magnetic field ($\mathbf{B}_\perp = \mathbf{e}_z \times \nabla \psi$) and for the stream function φ of the incompressible planar flow ($\mathbf{v}_\perp = \mathbf{e}_z \times \nabla \varphi$) [7]

$$\frac{\partial \psi}{\partial t} + [\varphi, \psi] = \eta(\nabla^2 \psi - J_0), \tag{1}$$

$$\frac{\partial \nabla^2 \varphi}{\partial t} + [\varphi, \nabla^2 \varphi] = [\psi, \nabla^2 \psi] + \nu \nabla^4 \varphi, \qquad (2)$$

where, following a standard notation, the convective terms are written as Jacobian operators ($[f,g] = \partial_x f \partial_y g - \partial_x g \partial_y f$). The above equations have been normalized with respect to the characteristic macroscopic length L, magnetic field $\bar{B}$, and Alfvén time $\tau_A = L/v_A$, while η and ν are, respectively, the inverse Lundquist number ($\eta c^2/4\pi v_A L$) and the inverse Reynolds number ($\nu/v_A L$). The Alfvèn velocity, $v_A = \bar{B}/(4\pi mn)^{1/2}$, is the velocity of small amplitude waves, propagating along the magnetic field $\bar{B}$ in a uniform plasma with density nm.

We will consider as basic equilibrium a magnetic shear in a motionless conducting fluid $\psi_0 = \mathcal{F}(x), \varphi_0 = 0$, where $\mathcal{F}$ is any function of a single coordinate. The forcing $J_0 = \nabla^2 \psi_0$ (magnetic energy input) balances the resistive term in Eq. (1). Notice that at the equilibrium the vorticity $\nabla^2 \varphi_0$ is not enhanced by the Lorentz force $[\psi_0, \nabla^2 \psi_0]$ in Eq. (2) due to the basic magnetic flux one dimensionality. For large values of resistivity and viscosity, this equilibrium is stable. At smaller values of the dissipation the only source of instability is in the nonlinear terms, whose effect will be shown on average to reduce to a renormalization of the molecular coefficients.

In the following we will choose $\mathcal{F}(x) = \cos x$ and we will work in a slab geometry with periodic boundary conditions. Such a configuration is widely used to study the evolution of large scale instabilities for its simplicity: any periodic function $\mathcal{F}(x)$ would fit. In this framework we will show that it is possible to evaluate analytically the renormalized resistivity and viscosity. It will turn out that eddy-resistivity can attain negative values which are the fingerprints of large scale instability.

III. MULTIPLE-SCALE ANALYSIS

We are interested in the evolution of perturbations which develop on a length scale (say L_{box}) much larger than the basic magnetic flux typical scale L. To this purpose, we can exploit the separation of scales as a perturbative parameter $[\varepsilon = O(L/L_{\text{box}})]$ and recast Eqs. (1),(2) in a multiple-scale form by introducing a set of *slow* variables ($X = \varepsilon x, Y = \varepsilon y, T = \varepsilon^2 t$) in addition to the *fast* variables (x,y,t) on which the basic flow evolves. The new variables have to be considered independent of the fast variables. Accordingly, the differential operators appearing in Eqs. (1),(2) are transformed into

$$\partial_i \rightarrow \partial_i + \varepsilon \nabla_i, \quad \partial_t \rightarrow \partial_t + \varepsilon^2 \partial_T, \qquad (3)$$

and the fields are expanded perturbatively in ε as

$$\psi = \psi^{(0)} + \varepsilon \psi^{(1)} + \varepsilon^2 \psi^{(2)} + \cdots, \qquad (4)$$

$$\varphi = \varphi^{(0)} + \varepsilon \varphi^{(1)} + \varepsilon^2 \varphi^{(2)} + \cdots, \qquad (5)$$

where $\psi^{(k)}$ and $\varphi^{(k)}$ depend on both fast (x,y,t) and slow (X,Y,T) variables. In the multiscale methods no prescription is given *a priori* for the ordering between the two sets of variables. Indeed, in this problem, the scaling of the slow

time T is suggested by physical hints: we are looking for a diffusive behavior of large scales which is supposed to take place on times of order $O(\varepsilon^{-2})$ (due to the eddy resistivity and viscosity). It is worth noticing that in general the large-scale MHD dynamics is first order in time and space (the well-known α effect) [5,8,9], but it can be shown that this is not the case for parity-invariant basic configurations [10].

By substituting Eq. (3) and Eqs. (4),(5) into Eqs. (1) and (2) and by equating the same powers of ε, one easily finds a hierarchy of equations in which perturbations belonging to different order of expansion appear coupled and depend on *fast* and *slow* variables. The dependence on the fast time variables can be discarded by observing that it reduces to a transient not affecting the long-time behavior, thanks to the fact that the forcing and the basic flux are time independent (a rigorous proof needs the construction of a Poincaré inequality) [11].

At each order in ε, we have an equation in which both fast and slow variables appears. We look for solutions with the same periodicities as the basic equilibrium. The dependence on the fast variable is then filtered out by averaging over the x-y periodicity. In this way we end up with a set of equations involving the large scale fields

$$\Psi^{(k)}(X,Y,T) = \langle \psi^{(k)} \rangle_{x,y}, \quad \Phi^{(k)}(X,Y,T) = \langle \varphi^{(k)} \rangle_{x,y}.$$

The equations have to be solved recursively because solutions of lower order appear as coefficients in the following steps of the hierarchy. In Appendix A we give a more detailed description of the procedure we followed. Briefly, we can here anticipate that the equation for the large scale magnetic flux $\Psi^{(0)}$ is obtained as solvability condition at order ε^2, while the equation for the large scale vorticity $\nabla^2 \Phi^{(0)}$ comes out at order ε^4

$$\frac{\partial \Psi^{(0)}}{\partial T} + [\Phi^{(0)}, \Psi^{(0)}] = \eta \nabla^2 \Psi^{(0)} - \frac{1}{2\nu} \frac{\partial^2 \Psi^{(0)}}{\partial Y^2}, \qquad (6)$$

$$\frac{\partial \nabla^2 \Phi^{(0)}}{\partial T} + [\Phi^{(0)}, \nabla^2 \Phi^{(0)}]$$

$$= [\Psi^{(0)}, \nabla^2 \Psi^{(0)}] + \frac{1}{2} \frac{\partial^2}{\partial X \partial Y} \left\{ \frac{1}{\nu^2} \left(1 + 2\frac{\nu}{\eta} \right) \left(\frac{\partial \Psi^{(0)}}{\partial Y} \right)^2 \right.$$

$$\left. + \frac{1}{\eta^2} \left(\frac{\partial \Phi^{(0)}}{\partial Y} \right)^2 \right\} + \frac{1}{2\eta} \frac{\partial^2}{\partial Y^2} \left(\frac{\partial^2}{\partial Y^2} - 3\frac{\partial^2}{\partial X^2} \right) \Phi^{(0)}$$

$$+ \nu \nabla^4 \Phi^{(0)}. \qquad (7)$$

Let us focus our attention on diffusive terms in Eqs. (6) and (7): as a consequence of the anisotropy of the basic small-scale flow the eddy diffusivities are anisotropic too. For longitudinal perturbations $[\Phi^{(0)} = \Phi^{(0)}(X,T), \Psi^{(0)} = \Psi^{(0)}(X,T)]$ both viscosity and resistivity are left unchanged. On the other hand, for transverse perturbations $[\Phi^{(0)} = \Phi^{(0)}(Y,T), \Psi^{(0)} = \Psi^{(0)}(Y,T)]$ the renormalization of resistivity due to the small scale magnetic energy holds a negative term ($-1/2\nu$), while molecular viscosity is increased by the eddy contribution ($1/2\eta$). From a general point of view, the multi-scale procedure eliminates all the contributions involving fast variables. The couplings be-
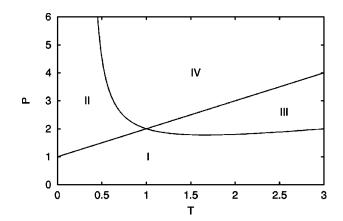
FIG. 1. Marginal stability lines for magnetic flux and stream function. Region I: stable with $\Gamma_\Psi < 0$ and $\Gamma_\Phi < 0$. Region II: $\Gamma_\Psi > 0$, $\Gamma_\Phi < 0$. Region III: $\Gamma_\Psi < 0$, $\Gamma_\Phi > 0$. Region IV: instable with $\Gamma_\Psi > 0$, $\Gamma_\Phi > 0$.

tween fast and slow components in the nonlinear terms are transformed into a renormalization of the molecular coefficients and in the new nonlinear terms in Eqs. (6),(7).

Linear stability analysis is performed by assuming a large scale perturbation of the type $\Psi^{(0)} \sim \exp(\Gamma_\Psi T + \iota K_X X + \iota K_Y Y)$ and $\Phi^{(0)} \sim \exp(\Gamma_\Phi T + \iota K_X X + \iota K_Y Y)$. The dispersion relations read

$$\Gamma_\Psi = -\eta K_X^2 - \left(\eta - \frac{1}{2\nu}\right)K_Y^2, \tag{8}$$

$$\Gamma_\Phi = -\frac{1}{K^2}\left[\left(\nu + \frac{1}{2\eta}\right)K_Y^4 + 2\left(\nu - \frac{3}{4\eta}\right)K_X^2 K_Y^2 + \nu K_X^4\right]. \tag{9}$$

The stability problem can be rephrased in simpler form by introducing the parameters $P = 1/2\eta\nu$ and $T = (K_X/K_Y)^2$. Marginal stability lines ($\Gamma_\Psi = \Gamma_\Phi = 0$) are then given by the equations

$$1 - P + T = 0, \tag{10}$$

$$1 + P + 2\left(1 - \frac{3}{2}P\right)T + T^2 = 0, \tag{11}$$

and are plotted in Fig. 1. For high enough values of molecular resistivity and viscosity ($P < 1$), the basic flow is stable against any large scale perturbation. Increasing the Reynolds numbers, the first instability sets in at $P = 1$ and $T = 0$, i.e., for transverse perturbations. We notice that for $1 < P < 16/9$ the large scale vorticity is always stable ($\Gamma_\Phi < 0$) and the magnetic potential growth rate Γ_Ψ is maximum in the case $T = 0$.

The large scale equations (6),(7) are actually more complicated than the original ones. In order to have an insight of the phenomenology of the large-scale dynamics, it is useful to limit ourselves to the situation of marginal instability in the neighborhood of the critical point ($P = 1, T = 0$).

IV. NONLINEAR EVOLUTION AT MARGINAL INSTABILITY

Special attention deserves the development of this large scale instability for Reynolds numbers close to the marginal stability threshold. In this regime we will see that the large scale equations became substantially simpler and it is possible to draw analytically conclusions concerning the nonlinear behavior. The final state is a fixed point characterized by a magnetic island of the size of the box. Numerical simulations indicate that this picture survive even for higher values of the Reynolds numbers.

The nonlinear evolution in the marginal regime is described by two coupled equations which generalize the Cahn-Hilliard equation, found for the hydrodynamical counterpart of this system, the so-called Kolmogorov flow [10,12,13]. Let us suppose to move the parameters just above the marginal stability line

$$\eta = \eta_c(1 - \varepsilon^2), \quad \nu = \nu_c(1 - \varepsilon^2), \tag{12}$$

where $\eta_c \nu_c = 1/2$ ($P = 1$). The perturbative parameter ε is thus fixed by the distance between η, ν and their critical values η_c, ν_c. We will take into account only transverse perturbations (i.e., without dependence on X) since, as shown in Fig. 1, the large scale magnetic flux linear instability is mainly transverse, close to $P = 1$. According to Eq. (6), the transverse eddy-resistivity in the neighborhood of the critical line defined by Eq. (12) is of order $O(\varepsilon^2)$, thus suggesting a scaling for the slow time $T = \varepsilon^4 t$. The decomposition rules (3) become

$$\partial_x \to \partial_x \quad \partial_y \to \partial_y + \varepsilon\partial_Y, \quad \partial_t \to \partial_t + \varepsilon^4 \partial_T. \tag{13}$$

The same multiscale technique described above can be adopted to solve perturbatively Eqs. (1) and (2). At first order in ε we obtain

$$\psi = \cos x + \Psi^{(0)}(Y,T) + \varepsilon\Psi^{(1)}(Y,T), \tag{14}$$

$$\varphi = 2\eta_c\varepsilon\frac{\partial\Psi^{(0)}}{\partial Y}\sin x. \tag{15}$$

We notice that the large scale stream function is linearly stable and it is simply driven by the magnetic flux perturbation $\Psi^{(0)}$. Averaging the equations over the fast variables, the evolution equations for $\Psi^{(0)}$ and $\Psi^{(1)}$ emerge at order ε^4 and ε^5, respectively,

$$\partial_T\Psi^{(0)} = -\frac{27}{8}\eta_c\partial_{4Y}\Psi^{(0)} - 2\eta_c\partial_{YY}\Psi^{(0)}$$
$$+ 12\eta_c\partial_{YY}\Psi^{(0)}(\partial_Y\Psi^{(0)})^2, \tag{16}$$

$$\partial_T\Psi^{(1)} = -\frac{27}{8}\eta_c\partial_{4Y}\Psi^{(1)} - 2\eta_c\partial_{YY}\Psi^{(1)}$$
$$+ 12\eta_c\partial_{YY}\Psi^{(1)}(\partial_Y\Psi^{(0)})^2$$
$$+ 24\eta_c\partial_Y\Psi^{(0)}\partial_{YY}\Psi^{(0)}\partial_Y\Psi^{(1)}. \tag{17}$$

In the first equation (16), one easily recognizes the renowned Cahn-Hilliard equation [12], which may be written in variational form

$$\frac{\partial \Psi^{(0)}}{\partial t} = - \frac{\delta V[\Psi^{(0)}]}{\delta \Psi^{(0)}}.$$

The existence of the Lyapunov functional

$$V[\Psi^{(0)}] = \eta_c \int dY \left[-(\partial_Y \Psi^{(0)})^2 + (\partial_Y \Psi^{(0)})^4 \right.$$
$$\left. + \frac{27}{16} (\partial_{YY} \Psi^{(0)})^2 \right] \qquad (18)$$

indicates that asymptotically the solution of Eq. (16) in a bounded domain reaches a fixed point. This stationary solution is approached by a sequence of metastable states of decreasing dominating mode. We thus expect to observe a non-linear evolution dominated by a magnetic island coalescence, analogous to the vortex pairing in 2D hydrodynamics [13].

Equation (17) is linear in $\Psi^{(1)}$, with coefficients depending nonlinearly on $\Psi^{(0)}$. It also can be written as a gradient flow, with a Lyapunov functional

$$V[\Psi^{(1)}] = \eta_c \int dY \left[-(\partial_Y \Psi^{(1)})^2 + 6(\partial_Y \Psi^{(0)})^2 (\partial_Y \Psi^{(1)})^2 \right.$$
$$\left. + \frac{27}{16} (\partial_{YY} \Psi^{(1)})^2 \right]. \qquad (19)$$

We conclude this section by observing that the dispersion relation for $\Psi^{(0)} \sim \exp(\Gamma T + \iota K Y)$ now reads

$$\Gamma = -\frac{27}{8} \eta_c K^4 + 2 \eta_c K^2. \qquad (20)$$

It implies instability ($\Gamma > 0$) for any $K \lesssim 0.77$. We notice that information about the characteristic scale of unstable modes was absent in the general treatment presented in the previous section because at any finite distance from the instability line, all the large scale modes are unstable.

V. NUMERICAL RESULTS

The analytical results presented in the previous section have been checked by extensive direct numerical simulations of MHD equations (1),(2). In order to force a transverse perturbation, we integrate the equations on a rectangular slab with $L = L_x = 2\pi$ and $L_y \geqslant L_x$. According to the notation used at the beginning of Sec. III, a large scale instability can only develop on the y direction for an aspect ratio $r = L_x/L_y < 1$.

Given the numerical values of parameters η and ν, from Eq. (12) and the condition $\eta_c \nu_c = 1/2$ we have

$$\varepsilon = \sqrt{1 - \sqrt{2 \eta \nu}}, \quad \eta_c = \sqrt{\frac{\eta}{2\nu}}, \qquad (21)$$

which are used for the theoretical predictions of the previous section.

The simplest check of our results concerns the growth rates of the instability which, in the initial linear regime, are given by the dispersion relation (20). In physical (not rescaled) variables (20) becomes
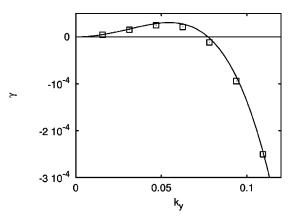

FIG. 2. Growth rates γ of the transverse Fourier modes k for simulation with $r = 1/64$, $\nu = 0.49$, and $\eta = 1.0$. The continuous line represents the linear prediction (22).

$$\gamma = -\frac{27}{8} \eta_c k^4 + 2 \eta_c \varepsilon^2 k^2, \qquad (22)$$

which shows that the largest unstable wave number is $k_{max} \simeq 0.77 \varepsilon$. The smallest transverse wave number is $k_1 = r$ thus, in order to numerically observe the instability, it must be $r \leqslant 0.77 \varepsilon$.

In Fig. 2 we report the growth rates of the first modes for a simulation with $r = 1/64$, $\nu = 0.49$, and $\eta = 1$. From Eq. (21) we have $\varepsilon \simeq 0.1$ and thus, according to Eq. (22), only the first four modes are unstable. The initial perturbation is small, random and on all the first 20 modes, we are then able to observe also negative γ's (stable modes). The comparison with the linear prediction (22) is very good even if ε is not very small. The numerical data of Fig. 2 have been obtained by a linear fit of the logarithm of the mode amplitude versus time in the early stages of the simulation.

Let us now consider the nonlinear stage of the perturbation growth. We describe here a different simulation with $r = 1/16$ and $\varepsilon \simeq 0.32$ which was advanced for a very long lapse of time. The nonlinear evolution will ultimately lead to a fixed point by a succession of long lasting quasiequilibrium states of decreasing wave number. The evolution of the amplitudes of the first five transverse modes computed from the direct numerical simulation is plotted in Fig. 3. Notice that in
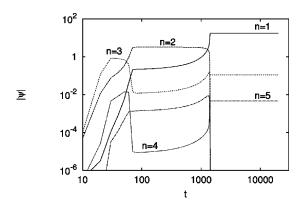

FIG. 3. Time evolution of magnetic potential of the first Fourier transverse components of wave number $k_n = n/16$ for the DNS with $r = 1/16$, $\eta = 0.4$, and $\nu = 1.0$. The number of unstable modes is 4.
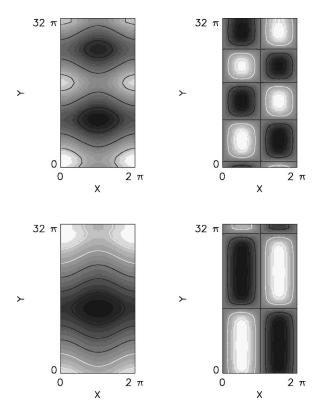
FIG. 4. Snapshot of the magnetic flux ψ (left) and stream function φ (right) for $t = 200$ (upper) and $t = 20\,000$ (lower).

FIG. 6. Snapshot of the stream function φ reconstructed according to Eq. (15) for $t = 200$ (left) and $t = 20\,000$ (right).

Hilliard equation for the large scale magnetic flux (16) with the same parameters of the DNS. As shown in Fig. 5 we find an impressive agreement even for very long times. The final relative amplitudes of the most energetic transverse modes is recovered within a 10% accuracy.

As a further test of the multiscale predictions, we checked the relations (14),(15) during the evolution. At leading order in ε, $\Psi^{(0)}(y,t)$ is obtained by subtracting the basic flow $\cos x$ from the magnetic flux $\psi(x,y,t)$. The resulting field, which reveals to be indeed x independent, is then used to reconstruct the stream function by means of Eq. (15). The results for the configuration of Fig. 4 is shown in Fig. 6.

this case the fifth mode $k = 5/16$ is linearly stable but it is nonlinearly driven by smaller wave number.

The typical linear time is now rather short, $1/\gamma \sim O(1)$, and the final stationary state, dominated by the largest available mode k_1, is reached at very long times, $t > 1000$. At intermediate times, almost stationary metastable states, characterized by decreasing leading mode, are punctuated by fast coalescence processes. Most of the energy dissipation takes place during these fast reconnection processes. In Fig. 4 we display the period-two metastable state at time $t = 200$ and the final, period-one state at $t = 20\,000$. The dynamical picture arising from Figs. 3 and 4 qualitatively agrees with the dynamics described by the Cahn-Hilliard equation [13].

To check quantitatively the validity of nonlinear multiscale analysis we have numerically integrated the Cahn-

VI. CONCLUSIONS

We have investigated the issue of stability of highly anisotropic, magnetic-energy dominated equilibrium states of the MHD fluid model equations. These configurations are known to be unstable for small values of resistivity leading to the formation of thin boundary layers in the nearby of the neutral line of the magnetic field [7,14]. At variance with the above case, we focused our attention on the range of moderate Lundquist/Reynolds numbers, where the boundary layer approximation is not fruitfully applicable. We have shown analytically, by means of multiple-scale analysis, that a type of large scale instability can arise above a definite threshold, and that for a generic perturbation the maximum growth is achieved by modes transverse to the magnetic field lines of the basic state. On the basis of this result, we have performed the multiple scale analysis for the marginally unstable case and for purely transverse perturbations. The analytic procedure yields a set of partial differential equations which describe the full nonlinear evolution of magnetic perturbations. It is possible to show that these equations possess a Lyapunov functional and thus their solutions asymptotically approach a fixed point which represents a nonlinear equilibrium different from the basic one. Direct numerical simulations of two-dimensional MHD performed with a pseudospectral code reveal an excellent *quantitative agreement* with the first-order analytical prediction in a wide range of values of the perturbative parameter. The development of large scale magnetic instabilities, caused by the occurrence of negative eddy diffusivities, is eventually related to inverse cascade of magnetic potential which is known to feature in two-dimensional MHD turbulence [15,16].
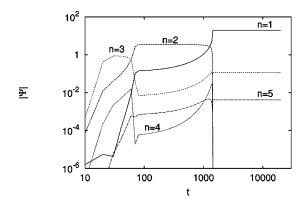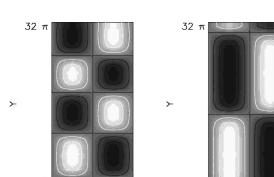

FIG. 5. Time evolution of the first square Fourier components of $\Psi^{(0)}$ solution of the Cahn-Hilliard equation. Compare with Fig. 3 relative to the direct numerical simulation of MHD equations.

Summarizing, the loss of stability of a magnetic shear at moderate Reynolds number is due to the growth of large scale perturbations whose main traits can be captured by a multiple scale analysis. When there is a single neutral line, at large enough Lundquist/Reynolds numbers, this mechanism is overcome by the formation of resistive boundary layers. The transverse large-scale instability here described is likely to be the generic mechanism of instability of sheared magnetic fields even for large Lundquist/Reynolds numbers whenever the basic state admits a large number of neutral lines.

APPENDIX: DERIVATION OF THE LARGE SCALE EQUATIONS

As anticipated in Sec. III, we give here a detailed description of the procedure we followed to derive the set of Eqs. (6),(7) governing the large scale dynamics. Since the algebra soon becomes heavy and nothing conceptually different happens for higher order terms, we limit ourselves to the second order in the expansion when Eq. (6) is found. We recall that the basic idea of multiple scale analysis (that of treating fast and slow variables independently) leads to the prescription

$$\partial_i \rightarrow \partial_i + \varepsilon \nabla_i, \quad \partial_t \rightarrow \partial_t + \varepsilon^2 \partial_T, \tag{A1}$$

for the differential operators appearing in MHD equations. As a first step, then, we substituted Eq. (A1) and the perturbative expansion

$$\psi = \psi^{(0)} + \varepsilon \psi^{(1)} + \varepsilon^2 \psi^{(2)} + \cdots,$$

$$\varphi = \varphi^{(0)} + \varepsilon \varphi^{(1)} + \varepsilon^2 \varphi^{(2)} + \cdots$$

in the MHD equations to yield two infinite sets of equations by equating to zero coefficients of different powers in ε. As the unknown fields $\psi^{(k)}(x,y,t;X,Y,T)$ and $\varphi^{(k)}(x,y,t;X,Y,T)$ are coupled hierarchically, these equations need to be solved recursively. It can be sufficient to look for functions with the same periodicity as the basic field.

To leading order, the equations simply read

$$-\eta \left(\frac{\partial^2 \psi^{(0)}}{\partial x^2} + \cos x \right) = 0,$$

$$-\nu \frac{\partial^4 \varphi^{(0)}}{\partial x^4} = 0$$

with solutions

$$\psi^{(0)}(x;X,Y,T) = \Psi^{(0)}(X,Y,T) + \cos x,$$

$$\varphi^{(0)}(x;X,Y,T) = \Phi^{(0)}(X,Y,T).$$

We notice here that at each step the solution will be given as the sum of a fluctuating (small scale) contribution and a mean (large scale) contribution, namely,

$$\Psi^{(k)}(X,Y,T) = \langle \psi^{(k)} \rangle_x, \quad \Phi^{(k)}(X,Y,T) = \langle \varphi^{(k)} \rangle_x.$$

At first order, the equations are

$$\frac{\partial \varphi^{(0)}}{\partial x} \frac{\partial \psi^{(0)}}{\partial Y} - \eta \frac{\partial^2 \psi^{(1)}}{\partial x^2} + 2 \frac{\partial^2 \psi^{(0)}}{\partial x \partial X} - \frac{\partial \varphi^{(0)}}{\partial Y} \frac{\partial \psi^{(0)}}{\partial x} = 0,$$

$$-\nu \frac{\partial^4 \varphi^{(1)}}{\partial x^4} + 4 \frac{\partial^4 \varphi^{(0)}}{\partial x^3 \partial X} - \frac{\partial \psi^{(0)}}{\partial x} \frac{\partial^3 \psi^{(0)}}{\partial x^2 \partial Y} + \frac{\partial \psi^{(0)}}{\partial Y} \frac{\partial^3 \psi^{(0)}}{\partial x^3}$$

$$- \frac{\partial \varphi^{(0)}}{\partial Y} \frac{\partial^3 \varphi^{(0)}}{\partial x^3} + \frac{\partial \varphi^{(0)}}{\partial x} \frac{\partial^3 \varphi^{(0)}}{\partial x^2 \partial Y} = 0.$$

As expected, the zeroth-order fields appear in the first order equation as coefficients. Substituting the solutions just found above, the two equations reduce to

$$-\eta \frac{\partial^2 \psi^{(1)}}{\partial x^2} + \frac{\partial \Phi^{(0)}}{\partial Y} \sin x = 0,$$

$$-\nu \frac{\partial^4 \varphi^{(1)}}{\partial x^4} + \frac{\partial \Psi^{(0)}}{\partial Y} \sin x = 0,$$

which can now be straightforwardly solved, leading to the first order fields

$$\psi^{(1)}(x;X,Y,T) = \Psi^{(1)}(X,Y,T) - \frac{1}{\eta} \frac{\partial \Phi^{(0)}}{\partial Y} \sin x,$$

$$\varphi^{(1)}(x;X,Y,T) = \Phi^{(1)}(X,Y,T) + \frac{1}{\nu} \frac{\partial \Psi^{(0)}}{\partial Y} \sin x.$$

Notice again that the solutions are well-behaved, since they have the required periodicity in the fast variables.

The same is not true for the solution of the magnetic flux function at second order. Consider in fact the equation

$$\frac{1}{\eta} \left(\frac{\partial \Phi^{(0)}}{\partial Y} \right)^2 \cos x - \frac{\partial \Phi^{(0)}}{\partial Y} \frac{\partial \Psi^{(0)}}{\partial X} + \frac{\partial \Phi^{(1)}}{\partial Y} \sin x$$

$$+ \frac{1}{\nu} \frac{\partial^2 \Psi^{(0)}}{\partial Y^2} \sin^2 x - \eta \frac{\partial^2 \Psi^{(0)}}{\partial Y^2} - \eta \frac{\partial^2 \psi^{(2)}}{\partial x^2}$$

$$+ \frac{1}{\nu} \left(\frac{\partial \Psi^{(0)}}{\partial Y} \right)^2 \cos x + 2 \frac{\partial^2 \Phi^{(0)}}{\partial X \partial Y} \cos x - \eta \frac{\partial^2 \Psi^{(0)}}{\partial X^2}$$

$$+ \frac{\partial \Psi^{(0)}}{\partial Y} \frac{\partial \Phi^{(0)}}{\partial X} + \frac{\partial \Psi^{(0)}}{\partial T} = 0, \tag{A2}$$

in which the lower order solutions have already been inserted. When integrated twice with respect to x to find $\psi^{(2)}$, it gives origin to secular terms, in fact proportional to x^2. In order to guarantee the periodicity conditions to be satisfied, we then have to impose that their sum is zero, namely

$$\frac{\partial \Psi^{(0)}}{\partial T} + [\Phi^{(0)}, \Psi^{(0)}] - \eta \nabla^2 \Psi^{(0)} + \frac{1}{2\nu} \frac{\partial^2 \Psi^{(0)}}{\partial Y^2} = 0.$$

This procedure (derive the equations, check for secular terms, impose solvability conditions, find the well-behaved solutions) has to be repeated up to the fourth order, when the evolution equation (7) for the large scale stream function $\Phi^{(0)}$ arises at last as a solvability condition.

Similarly, all the machinery is reproducible for the marginal unstable case, when the dissipative coefficients are expanded about the critical values η_c, ν_c. We used a symbolic manipulator software (MAPLE) to derive Eqs. (6),(7) and (16),(17).

[1] U. Frisch and S.A. Orszag, Phys. Today **1**, 24 (1990).
[2] L.D. Meshalkin and Ya.G. Sinai, J. Appl. Math. Mech. **25**, 1700 (1961).
[3] U. Frisch, B. Legras, and B. Villone, Physica D **96**, 36 (1996).
[4] A.V. Tur, A.V. Chechkin, and V.V. Yanovsky, Phys. Fluids B **4**, 3513 (1992).
[5] U. Frisch, in *Lecture Notes on Turbulence*, edited by J.R. Herring and J.C. McWilliams (World Scientific, Singapore, 1989), p. 234.
[6] D. Biskamp and U. Bremer, Phys. Rev. Lett. **72**, 3819 (1993).
[7] D. Biskamp, *NonLinear MagnetoHydroDynamics* (Cambridge University Press, Cambridge, England, 1993).
[8] F. Krause and K.H. Rädler, *Mean Field Magnetohydrodynam-ics and Dynamo Theory* (Pergamon Press, Oxford, 1980).
[9] H.K. Moffatt, *Magnetic Field Generation in Electrically Conducting Fluids* (Cambridge University Press, Cambridge, 1978).
[10] B. Dubrulle and U. Frisch, Phys. Rev. A **43**, 5355 (1991).
[11] L. Biferale, A. Crisanti, M. Vergassola, and A. Vulpiani, Phys. Fluids **7**, 2725 (1995).
[12] G. Sivashinky, Physica D **17**, 243 (1985).
[13] Z.S. She, Phys. Lett. A **124**, 161 (1987).
[14] H.P. Furth, J. Killen, and M.N. Rosenbluth, Phys. Fluids **6**, 459 (1963).
[15] A. Pouquet, J. Fluid Mech. **88**, 1 (1978).
[16] D. Biskamp, Plasma Phys. Controlled Fusion **26**, 311 (1984).